

LETTER • OPEN ACCESS

Simulated contribution of the interdecadal Pacific oscillation to the west Eurasia cooling in 1998–2013

To cite this article: Lingling Suo *et al* 2022 *Environ. Res. Lett.* **17** 094021

View the [article online](#) for updates and enhancements.

You may also like

- [The role of external forcing and internal variability in regulating global mean surface temperatures on decadal timescales](#)
Lu Dong and Michael J McPhaden
- [Drought variability in the eastern Australia and New Zealand summer drought atlas \(ANZDA, CE 1500–2012\) modulated by the Interdecadal Pacific Oscillation](#)
Jonathan G Palmer, Edward R Cook, Chris S M Turney *et al.*
- [The effectiveness of IPO institution reform in China: From the view of pricing efficiency changing and international comparison](#)
Ying Yu, Jiehao Shao and Ronghua Yi

ENVIRONMENTAL RESEARCH
LETTERS

LETTER

OPEN ACCESS

RECEIVED
28 April 2022REVISED
8 August 2022ACCEPTED FOR PUBLICATION
11 August 2022PUBLISHED
30 August 2022

Original content from
this work may be used
under the terms of the
[Creative Commons
Attribution 4.0 licence](#).

Any further distribution
of this work must
maintain attribution to
the author(s) and the title
of the work, journal
citation and DOI.

Simulated contribution of the interdecadal Pacific oscillation to
the west Eurasia cooling in 1998–2013Lingling Suo^{1,*} , Guillaume Gastineau², Yongqi Gao^{1,3}, Yu-Chiao Liang^{4,5,6} , Rohit Ghosh^{7,8}, Tian Tian⁹,
Ying Zhang³, Young-Oh Kwon⁶, Odd Helge Otterå¹⁰, Shuting Yang⁹ and Daniela Matei⁸¹ Nansen Environmental and Remote Sensing Center and Bjerknes Center for Climate Research, Bergen, Norway² UMR LOCEAN, Sorbonne Université, CNRS/IRD/MNHN, Paris, France³ Nansen-Zhu International Research Center, Institute of Atmospheric Physics, Chinese Academy of Sciences, 100029 Beijing, People's Republic of China⁴ Department of Atmospheric Sciences, National Taiwan University, Taipei, Taiwan⁵ Lamont-Doherty Earth Observatory, Columbia University, Palisades, NY, United States of America⁶ Woods Hole Oceanographic Institution, Woods Hole, MA, United States of America⁷ Department of Meteorology, University of Reading, Reading, United Kingdom⁸ Max Planck Institute for Meteorology, Hamburg, Germany⁹ Danish Meteorological Institute, Copenhagen, Denmark¹⁰ NORCE, Norwegian Research Centre AS, Bjerknes Centre for Climate Research, Bergen, Norway

* Author to whom any correspondence should be addressed.

E-mail: lingling.suo@nersc.no**Keywords:** interdecadal Pacific oscillation, Eurasia cooling, internal variabilitySupplementary material for this article is available [online](#)

Abstract

Large ensemble simulations with six atmospheric general circulation models involved are utilized to verify the interdecadal Pacific oscillation (IPO) impacts on the trend of Eurasian winter surface air temperatures (SAT) during 1998–2013, a period characterized by the prominent Eurasia cooling (EC). In our simulations, IPO brings a cooling trend over west-central Eurasia in 1998–2013, about a quarter of the observed EC in that area. The cooling is associated with the phase transition of the IPO to a strong negative. However, the standard deviation of the area-averaged SAT trends in the west EC region among ensembles, driven by internal variability intrinsic due to the atmosphere and land, is more than three times the isolated IPO impacts, which can shadow the modulation of the IPO on the west Eurasia winter climate.

1. Introduction

The long-term warming trend in the global mean surface temperature slowed down during 1998–2012/2013, the so-called ‘global warming hiatus’ (Easterling and Wehner 2009, Kosaka and Xie 2013). Further decomposing the global mean surface temperature trend into regions and seasons found that the reduction of the global warming rate is more dominant in boreal winter, with significant cooling across large parts of eastern North America and Eurasia (Cohen *et al* 2012, Li *et al* 2015).

Interdecadal Pacific oscillation (IPO) is proposed as one possible key factor causing the warming hiatus: when IPO is in its negative phase and presents a substantial negative trend, as it did in the 2000s, it

has the potential to produce a slowdown or pause in the observed global warming (Dong and Dai 2015, Steinman *et al* 2015, Meehl *et al* 2016, Zhang 2016, Gastineau *et al* 2019). Several studies further pointed out that the contribution of the equatorial Pacific surface cooling itself, which is the tropical part of the negative IPO, counteracted the global mean surface temperature rising caused by external radiative forcing to a large extent (Kosaka and Xie 2013, England *et al* 2014). However, the simulated Eurasia winter surface air temperature (SAT) trend in response to tropical Pacific sea surface temperature (SST) can be considerably diverse: Kosaka and Xie (2013) failed to reproduce the winter Eurasia cooling (EC), the non-negligible component of global warming hiatus, and the positive sea level pressure (SLP) anomalies over

Siberia; and in another study, a small fraction of ten members simulated by one model presented EC close to the reality while no EC found in another model's ten simulation members (Deser *et al* 2017), which implies the simulation of EC might be model dependent and (or) largely dominated by the internal atmospheric variability (Ogawa *et al* 2018).

EC culminated during the cold winters in 2010–2013, when the Pacific decadal oscillation, the northern Pacific expression of the IPO, was in the negative phase in the observations (Koenigk and Fuentes-Franco 2019). It is worth verifying if the north part of the IPO, in addition to the tropical part, might play a more significant role in phasing the Eurasia winter climate.

This manuscript explores the IPO impacts on the winter Eurasia climate in 1998–2013. The impacts of the pan-Pacific SST changes associated with IPO are isolated and compared with the internal variability. Large ensemble (>100) simulations from six atmospheric general circulation models (see section 2) are analyzed, which can reduce the model dependency and better evaluate the internal variability. Moreover, the internal variability can be largely eliminated in the ensemble mean.

2. Methods

ECMWF Reanalysis v5 (ERA5) dataset (Hersbach *et al* 2020) is used to compare with the model output. Two sets of large-ensemble experiments (table 1), both performed with six state-of-the-art atmosphere general circulation models, are analyzed in this work. The first one is the experiment (hereafter ALL refers to experiment 1) starting from 1 January 1979 using prescribed daily SST and sea ice concentration from the HadISST 2.0 (Titchner and Rayner 2014) as boundary conditions and with the external forcing from HighResMIP (Haarsma *et al* 2016) in IPSL-CM6 or CMIP6 (Eyring *et al* 2016) in other models. The external radiative forcings in HighResMIP are identical to CMIP6, except for the anthropogenic aerosol optical depth and effective radius deltas (see table 1 in Haarsma *et al* 2016). The second experiment is the same as ALL, but with the IPO signals removed from the daily SST in the Pacific Ocean (hereafter NoIPO refers to experiment 2). The difference of the experiments ALL minus NoIPO estimates the influence of the IPO, accounting for interactions with the external forcings changes and the other mode of internal variability (Hua *et al* 2018, Wang 2019).

The IPO data, which is calculated from the ERSSTv4 (Huang *et al* 2016) and downloaded from the Decadal Climate Prediction Project (Boer *et al* 2016) panel of CMIP6. The method adopted to calculate the IPO and the associated patterns is given

Table 1. Summary of the models used in this study and the number of members for each experiment. For the technical details of each model, please refer to table 1 in Liang *et al* (2021).

	ALL	NoIPO
CAM6-Nor (Seland <i>et al</i> 2020)	30	20
EC-EARTH3 (Döscher <i>et al</i> 2022)	20	20
ECHAM6.3 (Stevens <i>et al</i> 2013)	10	10
IAP4 (Zhang <i>et al</i> 2013)	15	15
IPSL-CM6 (Hourdin <i>et al</i> 2020)	30	20
WACCM6 (Gettelman <i>et al</i> 2019)	30	30
Total of ensembles	135	115

at www.wcrp-climate.org/wgsip/documents/Tech-Note-1.pdf. The method first estimates the effect of the external radiative forcing using the first signal to noise maximizing Empirical Orthogonal Functions (Ting *et al* 2009) from the CMIP5 multi-model ensemble. The historical simulation before 2005 and the representative concentration pathway 8.5 simulation after 2013 are used. After subtracting the effect of the external forcing from the SST data, the residual SST represents the internal variability. Empirical orthogonal function analysis is then conducted using the residual SST in the Pacific basin from 40° S to 60° N. The IPO time series is defined as the low pass filtered first principal component, using a second order Butterworth filter with a cutoff period of 13 years. The IPO pattern is given by the regression on the IPO time series of the residual SST. The reconstructed IPO variability, given by the multiplication of the pattern and the index at a given time step, is then interpolated at the monthly time step and on the HadISST 2.0 horizontal grid. Such reconstructed IPO is subtracted from the HadISST 2.0 data to produce the SST prescribed in NoIPO. Alternative IPO definitions were tested, and led to a similar pattern and time series (supplementary material table S1).

Trends in the ERA5 and each member of the simulations are computed by a least-squares fit of the linear regression. A two-tailed t-test verifies the statistical significance of the trend with a null hypothesis that the trend is zero (Santer *et al* 2000). The trend is statistically significant at the 5% level when the corresponding probability value is less than 0.05. The IPO impacts are obtained by subtracting the ensemble mean of the NoIPO from that of the ALL. The independent two-sample t-test is used to examine whether the differences (impacts) are statistically significant with a stipulated significance level at 0.05 (Santer *et al* 2000).

The probability density function (PDF) of the area-averaged SAT trends over the EC region is estimated using the kernel density estimation method from the ensemble members. The winter season is concerned in this work. A winter includes the

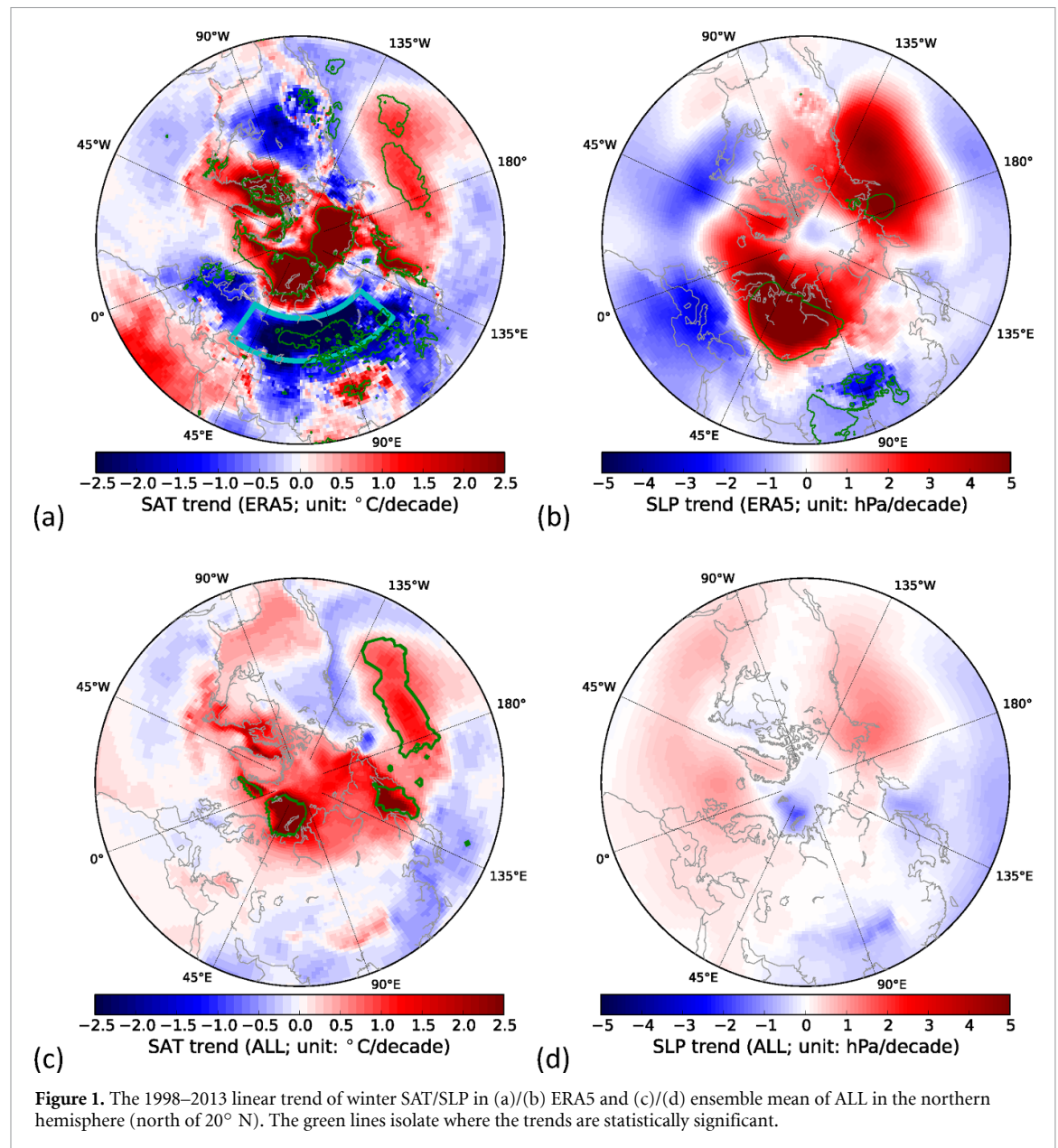


Figure 1. The 1998–2013 linear trend of winter SAT/SLP in (a)/(b) ERA5 and (c)/(d) ensemble mean of ALL in the northern hemisphere (north of 20° N). The green lines isolate where the trends are statistically significant.

previous year's December and the current year's January–February.

3. Results

3.1. Role of the IPO

The 1998–2013 linear trends of winter SAT in ERA5 present an extensive cooling along the whole mid-latitudes Eurasia in which the mid-eastern EC are statistically significant, and a statistically significant prominent warming over the Arctic and the central North Pacific (figure 1(a)), in agreement with previous studies (Zhang *et al* 2012, Li *et al* 2015). The cooling trends over most of central Eurasia exceed 2.5 °C/decade during 1998–2013. There are two highs in SLP trends located in the Siberia regions and the North Pacific associated with the SAT patterns

(figure 1(b)). The results in the observation datasets HadCRU5 (Morice *et al* 2021) and HadSLP2r (Allan and Ansell 2006) also confirm the SAT and SLP trend patterns shown in ERA5 (supplementary material figure S1).

The ensemble mean of ALL (figure 1(c)) reproduces the North Pacific warming well, the Arctic warming with reduced intensity over the East Siberian Sea and the Chukchi Sea but shows a total absence of the strong cooling over central Eurasia. The SLP trends in ALL are much weaker than ERA5 and are not statistically significant in the Northern Hemisphere (figure 1(d)). The ensemble mean largely removes the internal variability intrinsic due to the atmosphere and land (IV-AL) as SST and sea ice are prescribed in the boundary conditions in our simulations. The absence of EC in ALL implies that IV-AL

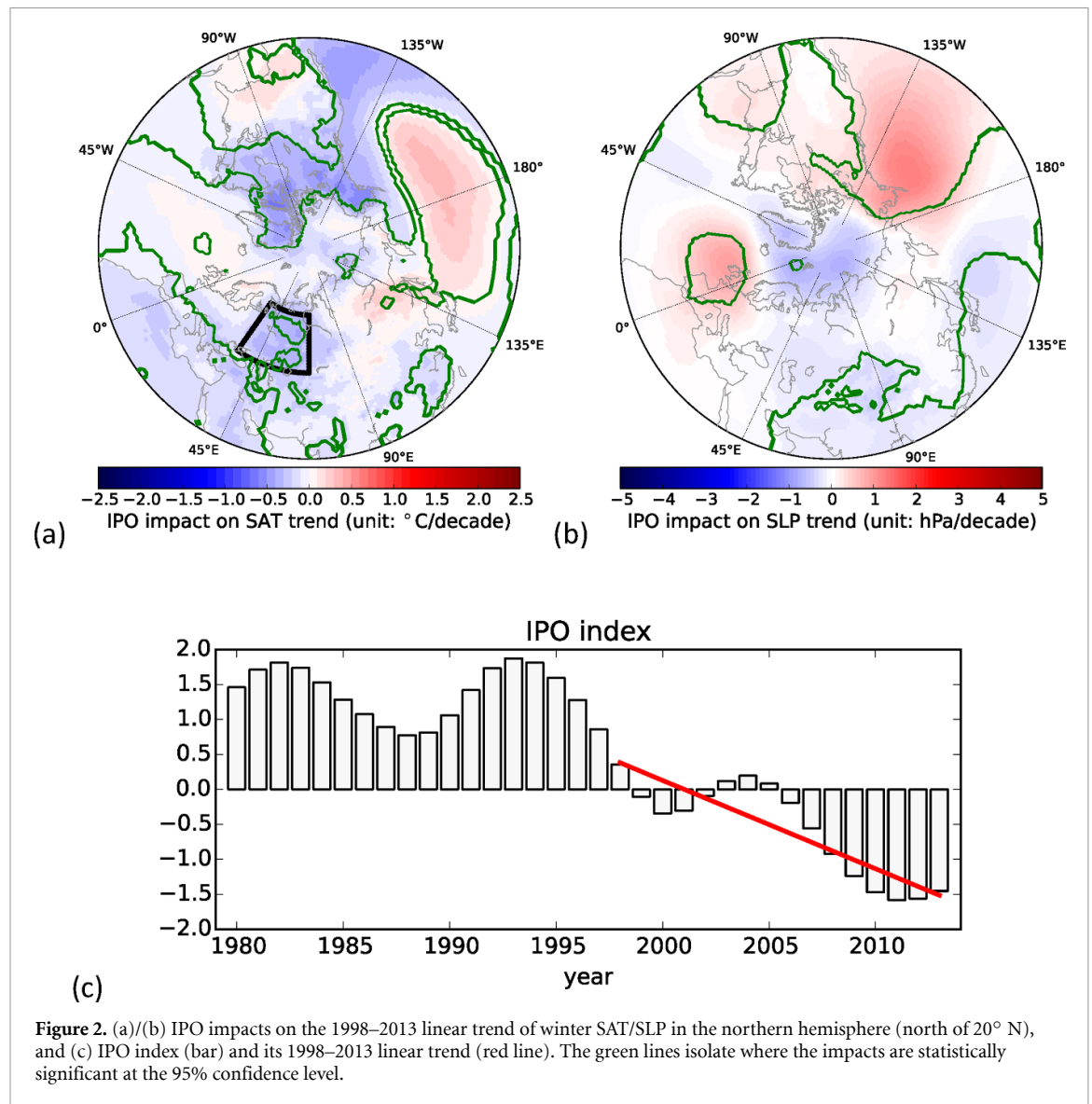


Figure 2. (a)/(b) IPO impacts on the 1998–2013 linear trend of winter SAT/SLP in the northern hemisphere (north of 20° N), and (c) IPO index (bar) and its 1998–2013 linear trend (red line). The green lines isolate where the impacts are statistically significant at the 95% confidence level.

might be a dominant factor in causing the observed EC, which agrees with previous studies (Li *et al* 2015, Ogawa *et al* 2018). It can also be due to deficiency in the climate models to represent mid-latitude climate change (Stevens and Bony 2013, Shepherd 2014) or uncertainties related to the SST/SIC and external forcing used (Cheung *et al* 2022). The diversity of EC driven by IV-AL will be evaluated and discussed in part 3.2.

The impacts of the IPO are isolated as the difference between ALL and NoIPO. The IPO brings a statistically significant winter cooling over west-central Eurasia (marked by the black frame in figure 2(a)) in 1998–2013. The cooling rate is up to around 0.4 °C–0.5 °C/decade, accompanied by a warming trend over the west-mid north Pacific. In this period, the SLP trends driven by the IPO are statistically significant positive over the North Pacific, so that the Aleutian Low weakens. Statistically significant positive SLP trends are also located over the northeast Atlantic. Negative trends are simulated over the Arctic but

with only a limited level of significance (figure 2(b)). The low-pressure anomalies situated over the Arctic and the high over the northeast Atlantic can drive more cold airflow across Scandinavia to west-central Eurasia, which causes the cooling there.

Such SAT and SLP responses are associated with a declining trend of the IPO index in 1998–2013 (figure 2(c)). The positive (negative) IPO phase is associated with an intensified (weakened) Aleutian Low in winter (Mantua and Hare 2002). With the IPO changing from a weakly positive to a strongly negative phase in 1998–2013, the Aleutian Low has weakened. The teleconnection of the weakened winter Aleutian Low in the negative IPO phase far reaches the northeast Atlantic with an anomalous high there, which has already been presented by previous studies (Kren *et al* 2016, Elsberry *et al* 2019).

3.2. Evaluation of the internal variability

The simulated IPO impacts over Eurasia are much weaker than the observed EC in ERA5. Therefore, we

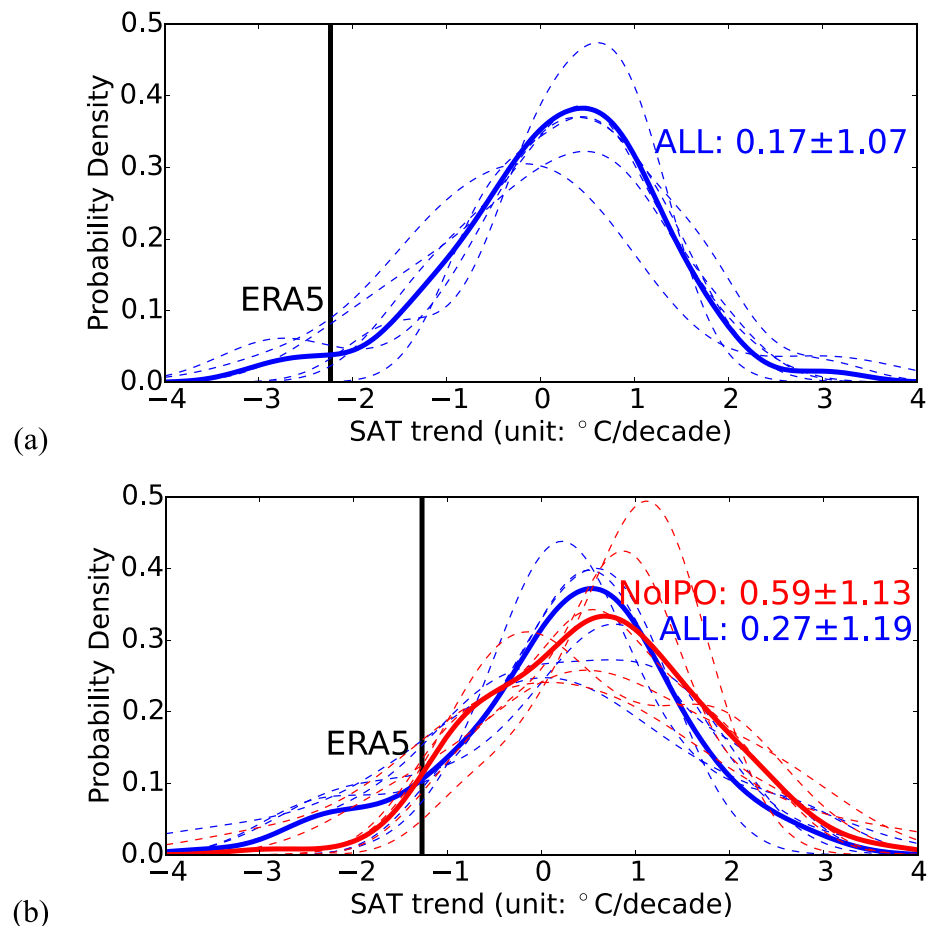


Figure 3. PDFs of 1998–2013 SAT trend averaged over (a) 35° E–120° E and 45° N–60° N and (b) 35° E–70° E and 45° N–65° N (the region enclosed by the cran frame in figure 1(a) and black frame in figure 2(a)) estimated from ALL/NoIPO ensembles (blue/red lines). The thin dotted lines show the PDFs estimated from the single model ensembles, and the thick lines show the PDFs estimated from all model ensembles. Blackline marks the respective corresponding average in ERA5. Numbers indicate the mean \pm standard deviation of the ensemble distributions.

quantify the potential of IV-AL in driving the EC. The large ensemble used has the advantage of better evaluating the IV-AL.

First, the ensemble distribution of EC in ALL is compared with ERA5. Figure 3(a) shows the estimated PDFs of the 1998–2013 SAT trend averaged over the EC region (35° E–120° E and 45° N–60° N, the region enclosed by the cran frame in figure 1(a)) from ALL. The ensemble mean of ALL (0.17 °C/decade) fails in reproducing the EC, but the EC in ERA5 (−2.24 °C/decade) does locate inside the ALL distribution coverage. Five members from three models out of 135 in ALL, as a percentage of 3.7%, reproduce a stronger EC than ERA5, while none found in the NoIPO members. The five members present the key features of the observed EC with the Barents–Kara seas warming and the extensive cooling along Eurasia, and the strong positive SLP trends over the Ural blocking regions (figure 4). This indicates that IV-AL, together with the IPO, has the ability to drive the EC.

Then the role of the IPO is compared with the IV-AL. Figure 3(b) shows the estimated PDFs of the 1998–2013 SAT trend averaged over the region

with significant IPO impacts (35° E–70° E and 45° N–65° N, the region enclosed by the black frame in figure 2(a)), which is the west part of the EC region, with the north border shifted 5° further north. When IPO signals are removed, the distribution of the trends among ensembles moves toward positive, with the mean from 0.27 °C/decade in ALL to 0.59 °C/decade in NoIPO. The difference between the mean in ALL and NoIPO is statistically significant. The IPO impact (0.32 °C/decade) is 25.2% of the observed west EC in ERA5 (1.27 °C/decade). There are 13 members from four models (9.63%) in ALL showing stronger west EC than ERA5, while only three members (2.61%) from two models are found in the NoIPO ensemble. This again supports the conclusion that IPO contributed to the west EC in 1998–2013. However, the standard deviation of the trends in all members is 1.19 °C/decade in ALL and 1.13 °C/decade in NoIPO, about 3.5–3.7 times the IPO impact. This illustrates that the IV-AL might overshadow the IPO role in driving the EC. And it could be difficult to isolate the IPO impacts in small ensemble simulations.

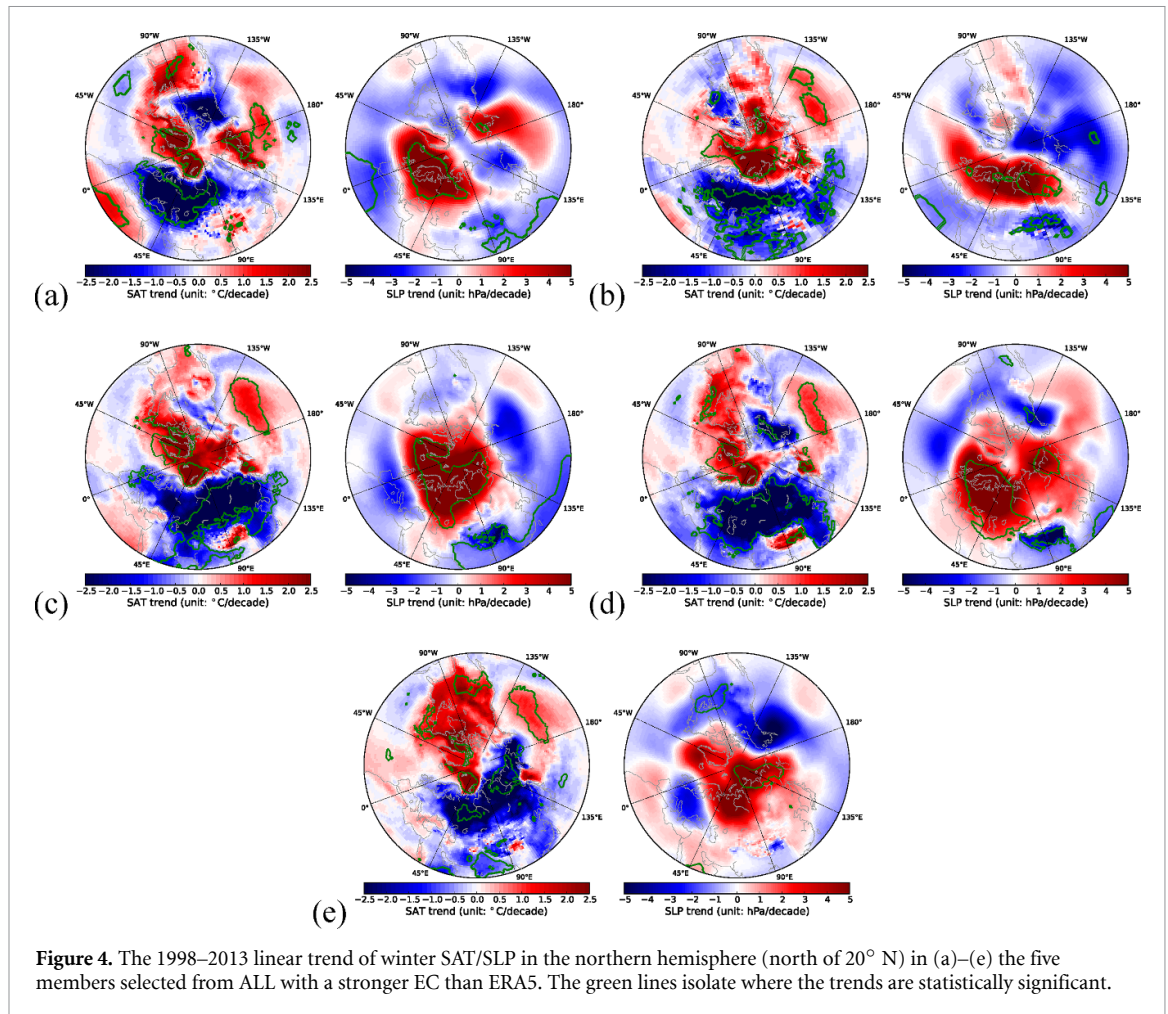


Figure 4. The 1998–2013 linear trend of winter SAT/SLP in the northern hemisphere (north of 20° N) in (a)–(e) the five members selected from ALL with a stronger EC than ERA5. The green lines isolate where the trends are statistically significant.

4. Conclusion and discussion

In our coordinated multi-model large ensemble simulations, the internally driven IPO brings a cooling trend over the west part of the EC region during 1998–2013. The cooling driven by IPO is about a quarter of the observed EC in this area. The cooling trend is associated with the phase transition to the strong negative IPO, which drives SLP changes with positive/negative/positive SLP trends situated over the North Pacific/Arctic/Northeast Atlantic regions.

The internal variability intrinsic due to the atmosphere and land is also evaluated using the large ensembles. The EC/west-EC shown in ERA5 is located at the 3.7th/9.63th percentile of the ALL distribution. The spread among ensembles driven by internal variability is more than three times the isolated IPO impacts, which can shadow the modulation of the IPO on the west Eurasia winter climate.

Based on the results presented in this study, the IPO can be expected to reduce the severely cold winters in the west Eurasia regions when it reversed to its positive phase. Still, this hypothesis needs to be verified by further study. This study concerns the internal-driven IPO impact. The external radiative forcing can also alter the decadal SST variations in the

Pacific (Meehl *et al* 2013). When the decadal Pacific SST variations driven by external forcing are in or out of phase with the internally driven IPO, the impacts of the Pacific on Eurasia would be intensified or reduced. It would be useful to compare and also combine the impacts of internally and externally driven Pacific SST variations to improve the climate prediction in the Eurasia region.

Data availability statement


The data (Suo *et al* 2022) that support the findings of this study are openly available at the following URL/DOI: <http://ns9015k.web.sigma2.no/BlueAct/>.

Acknowledgments

This work is funded by the JPI Climate-Oceans ROADMAP and the Blue-Action Project (European Union's Horizon 2020 research and innovation program, 727852). The CAM6-Nor simulations were performed on resources provided by UNINETT Sigma2—the National Infrastructure for High Performance Computing and Data Storage in Norway (nn2343k, NS9015K). The simulations of IAP4.1 were

supported by National Key R&D Program of China 2017YFE0111800.

ORCID iDs

Lingling Suo  <https://orcid.org/0000-0003-2385-4730>

Yu-Chiao Liang  <https://orcid.org/0000-0002-9347-2466>

References

- Allan R and Ansell T 2006 A new globally complete monthly historical gridded mean sea level pressure dataset (HadSLP2): 1850–2004 *J. Clim.* **19** 5816–42
- Boer G J *et al* 2016 The decadal climate prediction project (DCPP) contribution to CMIP6 *Geosci. Model. Dev.* **9** 3751–77
- Cheung H *et al* 2022 Assessing the influence of sea surface temperature and arctic sea ice cover on the uncertainty in the boreal winter future climate projections *Clim. Dyn.* **59** 433–54
- Cohen J L, Furtado J C, Barlow M, Alexeev V A and Cherry J E 2012 Asymmetric seasonal temperature trends *Geophys. Res. Lett.* **39** L04705
- Deser C, Guo R and Lehner F 2017 The relative contributions of tropical Pacific sea surface temperatures and atmospheric internal variability to the recent global warming hiatus *Geophys. Res. Lett.* **44** 7945–54
- Dong B and Dai A 2015 The influence of the interdecadal Pacific oscillation on temperature and precipitation over the globe *Clim. Dyn.* **45** 2667–81
- Döscher R *et al* 2022 The EC-Earth3 earth system model for the coupled model intercomparison project 6 *Geosci. Model. Dev.* **15** 2973–3020
- Easterling D R and Wehner M F 2009 Is the climate warming or cooling? *Geophys. Res. Lett.* **36** L8706
- Elsbury D, Peings Y, Saint-Martin D, Douville H and Magnusdottir G 2019 The atmospheric response to positive IPV, positive AMV, and their combination in boreal winter *J. Clim.* **32** 4193–213
- England M H, McGregor S, Spence P, Meehl G A, Timmermann A, Cai W, Gupta A S, McPhaden M J, Purich A and Santoso A 2014 Recent intensification of wind-driven circulation in the Pacific and the ongoing warming hiatus *Nat. Clim. Change* **4** 222–7
- Eyring V, Bony S, Meehl G A, Senior C A, Stevens B, Stouffer R J and Taylor K E 2016 Overview of the coupled model intercomparison project phase 6 (CMIP6) experimental design and organization *Geosci. Model. Dev.* **9** 1937–58
- Gastineau G, Friedman A R, Khodri M and Vialard J 2019 Global ocean heat content redistribution during the 1998–2012 interdecadal Pacific oscillation negative phase *Clim. Dyn.* **53** 1187–208
- Gottelman A *et al* 2019 The whole atmosphere community climate model version 6 (WACCM6) *J. Geophys. Res.* **124** 12380–403
- Haarsma R J *et al* 2016 High resolution model intercomparison project (HighResMIP v1.0) for CMIP6 *Geosci. Model. Dev.* **9** 4185–208
- Hersbach H *et al* 2020 The ERA5 global reanalysis *Q. J. R. Meteorol. Soc.* **146** 1999–2049
- Hourdin F *et al* 2020 LMDZ6A: the atmospheric component of the IPSL climate model with improved and better tuned physics *J. Adv. Model. Earth Syst.* **12** e1892M–e2019M
- Hua W, Dai A and Qin M 2018 Contributions of internal variability and external forcing to the recent Pacific decadal variations *Geophys. Res. Lett.* **45** 7084–92
- Huang B, Thorne P W, Smith T M, Liu W, Lawrimore J, Banzon V F, Zhang H, Peterson T C and Menne M 2016 Further exploring and quantifying uncertainties for extended reconstructed sea surface temperature (ERSST) Version 4 (v4) *J. Clim.* **29** 3119–42
- Koenigk T and Fuentes-Franco R 2019 Towards normal Siberian winter temperatures? *Int. J. Climatol.* **39** 4567–74
- Kosaka Y and Xie S 2013 Recent global-warming hiatus tied to equatorial Pacific surface cooling *Nature* **501** 403–7
- Kren A C, Marsh D R, Smith A K and Pilewski P 2016 Wintertime Northern hemisphere response in the stratosphere to the Pacific decadal oscillation using the Whole Atmosphere Community Climate Model *J. Clim.* **29** 1031–49
- Li C, Stevens B and Marotzke J 2015 Eurasian winter cooling in the warming hiatus of 1998–2012 *Geophys. Res. Lett.* **42** 8131–9
- Liang Y *et al* 2021 Impacts of Arctic Sea ice on cold season atmospheric variability and trends estimated from observations and a multi-model large ensemble *J. Clim.* **34** 8419–43
- Mantua N J and Hare S R 2002 The Pacific decadal oscillation *J. Oceanogr.* **58** 35–44
- Meehl G A, Hu A, Arblaster J M, Fasullo J and Trenberth K E 2013 Externally forced and internally generated decadal climate variability associated with the interdecadal Pacific Oscillation *J. Clim.* **26** 7298–310
- Meehl G A, Hu A, Santer B D and Xie S 2016 Contribution of the Interdecadal Pacific Oscillation to twentieth-century global surface temperature trends *Nat. Clim. Change* **6** 1005–8
- Morice C P, Kennedy J J, Rayner N A, Winn J P, Hogan E, Killick R E, Dunn R J H, Osborn T J, Jones P D and Simpson I R 2021 An updated assessment of near-surface temperature change from 1850: the HadCRUT5 data set *J. Geophys. Res.* **126** e2019J–e32361J
- Ogawa F *et al* 2018 Evaluating impacts of recent Arctic sea-ice loss on the northern hemisphere winter climate change *Geophys. Res. Lett.* **45** 3255–63
- Santer B D, Wigley T M L, Boyle J S, Gaffen D J, Hnilo J J, Nychka D, Parker D E and Taylor K E 2000 Statistical significance of trends and trend differences in layer-average atmospheric temperature time series *J. Geophys. Res.* **105** 7337–56
- Seland Ø *et al* 2020 Overview of the Norwegian Earth system model (NorESM2) and key climate response of CMIP6 DECK, historical, and scenario simulations *Geosci. Model. Dev.* **13** 6165–200
- Shepherd T G 2014 Atmospheric circulation as a source of uncertainty in climate change projections *Nat. Geosci.* **7** 703–8
- Steinman B A, Mann M E and Miller S K 2015 Atlantic and Pacific multidecadal oscillations and Northern Hemisphere temperatures *Science* **347** 988
- Stevens B *et al* 2013 Atmospheric component of the MPI-M earth system model: ECHAM6 *J. Adv. Model. Earth Syst.* **5** 146–72
- Stevens B and Bony S 2013 What are climate models missing? *Science* **340** 1053–4
- Suo L *et al* 2022 Datasets for publication “Simulated contribution of the interdecadal Pacific oscillation to the west Eurasia cooling in 1998–2013” (available at: <http://ns9015k.web.sigma2.no/BlueAct/>)
- Ting M, Kushnir Y, Seager R and Li C 2009 Forced and internal twentieth-century SST trends in the North Atlantic *J. Clim.* **22** 1469–81
- Titchner H A and Rayner N A 2014 The Met Office Hadley Centre sea ice and sea surface temperature data set, version 2: 1. Sea ice concentrations *J. Geophys. Res.* **119** 2864–89
- Wang C 2019 Three-ocean interactions and climate variability: a review and perspective *Clim. Dyn.* **53** 5119–36
- Zhang H, Zhang M and Zeng Q 2013 Sensitivity of simulated climate to two atmospheric models: interpretation of differences between dry models and moist models *Mon. Weather Rev.* **141** 1558–76
- Zhang L 2016 The roles of external forcing and natural variability in global warming hiatuses *Clim. Dyn.* **47** 3157–69
- Zhang X, Lu C and Guan Z 2012 Weakened cyclones, intensified anticyclones and recent extreme cold winter weather events in Eurasia *Environ. Res. Lett.* **7** 044044